Available online at www.sciencedirect.com

ScienceDirect

Procedia CIRP 67 (2018) 191 – 196

www.elsevier.com/locate/procedia

11th CIRP Conference on Intelligent Computation in Manufacturing Engineering, CIRP ICME '17

On the effect of part orientation on stress distribution in AlSi10Mg specimens fabricated by laser powder bed fusion (L-PBF)

Alessandro Salmi[a,]*, Gabriele Piscopo[a], Eleonora Atzeni[a], Paolo Minetola[a], Luca Iuliano[a]

[a]*Politecnico di Torino, Department of Management and Production Engineering (DIGEP), C.so Duca degli Abruzzi, 24, 10129 Torino, Italy*

* Corresponding author. Tel.: +39-011-090-7210; fax: +39-011-090-7299. E-mail address: alessandro.salmi@polito.it

Abstract

The freedom of design of AM products suffers from some limitations in case of powder bed metal processes, because AM part's integrity is affected by the residual stress state that is a consequence of the thermal history during part fabrication. Aim of this work is to evaluate the effect of part orientation on stress distribution. Thus, flat samples of AlSi10Mg alloy built along different orientations are produced by means of laser powder bed fusion (L-PBF) process, also known as Selective Laser Melting (SLM). Then, the semi-destructive hole-drilling method is used to evaluate residual stresses beneath the surfaces of samples. The outcomes of the study can be exploited to define design rules in order to both minimize support structures and optimize the orientation of the part in the building volume.

Peer-review under responsibility of the scientific committee of the 11th CIRP Conference on Intelligent Computation in Manufacturing Engineering

Keywords: Residual stresses; Powder bed fusion; AlSi10Mg; Hole-drilling method; Orientation.

1. Introduction

Due to its potentialities, Additive manufacturing (AM) is actually being adopted by several industries to produce metal components, in particular prototypes or individual parts. In the aerospace and racing sectors, metal additive parts are yet fabricated in small batches of redesigned products, in order to take advantage of the complex and lightweight design that is possible to be produced with this technology, or to improve the performances of the components using materials that have been developed specifically for AM. With Industry 4.0, it is expected that the AM technology will be used consistently to produce final products for different applications and industries [1]. However, this step forward requires that AM processes and parts meet quality and repeatability standards that currently do not exist. Thus, efforts are being made by the scientific community to increase the knowledge on AM processes and the quality of parts.

Among the various AM technologies that are able to produce metal components, laser powder bed fusion (L-PBF), which is also known as Selective Laser Melting (SLM), has been applied extensively in different industrial sectors [2]. In the L-PBF process, metal powders are spread in thin layers onto a building platform and a laser beam is utilized to selectively melt the powder. Hence, layer-by-layer, parts of elevated geometrical complexity are fabricated [2]. It is recognized that manufacturing processes in which a laser is used as an energy source, such as soldering and laser bending, generate high levels of residual stresses, because of the large temperature gradients that are produced on the components [3,4]. In the case of the L-PBF process, the residual stresses are responsible of distortions, cracks and delamination between layers (Fig. 1), as well as detachments from support structures or even the failure of the AM process [5-9]. Moreover, the stress distribution on the final component can affect the integrity and lifetime of the part to a great extent.

The study of Mercelis and Kruth [10] theoretically and experimentally describes the development of residual stresses on the basis of the Temperature Gradient Mechanism (TGM). In details, the steep temperature gradient in the exposed area of the powder bed produces transient thermal deformations on the last layer and on the previous ones. When the laser source

Peer-review under responsibility of the scientific committee of the 11th CIRP Conference on Intelligent Computation in Manufacturing Engineering
doi:10.1016/j.procir.2017.12.198

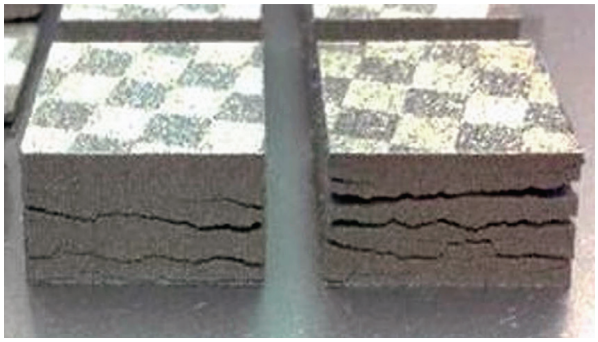

Fig. 1. Macroscopic distortion, cracking and delamination due to high values of residual stresses, that exceed the binding ability between the top layer and the previous ones [9].

is removed, the processed material cools down and shrinks more than the non-exposed material that is present in the surrounding areas, and residual stresses are thus created. Other studies by Gusarov *et al.* [11] highlight that longitudinal tensile stresses are on average two times greater than transversal ones. Using a thermo-elastic model, they could explain the formation of two longitudinal and transversal crack systems that were observed during model validation experiments. The exposure strategy, such as island scanning or rotation of the scan pattern between layers, of L-PBF machines can reduce residual stresses by shortening the scan tracks or creating a more uniform stress distribution as it compensates for directional anisotropy [12,13]. Besides, residual stresses are a consequence of material thermo-mechanical properties. The elastic modulus, the coefficient of thermal expansion (CTE) and the phase transformation phenomena are important factors that determine the residual stress level of the AM processed component [14].

Nevertheless, in the scientific literature most studies of residual stresses in L-PBF concern the process parameters, the scanning strategies, and the material properties. Very few studies are focused on the correlation between stress state and geometry and part orientation during building. Some works can be found in the literature that have had the aim of evaluating the residual stress distribution in the different longitudinal, transversal and normal directions, with reference to parallelepiped samples of thin walls, in order to simplify the analysis. Studies have been carried out on mild steel (grade S355JR-AR), 316 Stainless Steel and Inconel 718 samples [15-17]. Studies on residual stresses are of a qualitative or semi-quantitative type, and are based on the evaluation of the deformations of bridge or cantilever structures [18].

In this work, the process-induced residual stresses on AlSi10Mg components, fabricated by L-PBF, have been investigated using the hole drilling method, according to the ASTM E837-13a standard [19]. Flat specimens built along different orientations have been considered, in order to evaluate how stresses are altered by geometrical constraints. This experimental activity has made it possible to draw the trends of the residual stresses beneath the surfaces of samples produced in AlSi10Mg alloy, resulting from changes in the orientation of the part.

2. Materials and methods

The material that has been the subject of the investigations, the considered geometries and the manufacturing process of the samples are explained in detail in the subsequent sections. The methodology adopted to measure and evaluate the residual stresses is also illustrated briefly.

2.1. Material

AlSi10Mg alloy has been selected for this study. AlSi10Mg is a typical cast alloy that is used to produce complex geometries. Its use for AM applications allows complex low weight parts with good static, dynamic and thermal properties to be produced. Table 1 shows the main mechanical properties of this material, according to Manfredi *et al.* [20] experimental investigation on material characterization.

2.2. Geometries

In order to evaluate the influence of the part orientation on the residual stresses induced by the L-PBF process, nine specimens have been considered. These are all flat specimens with a small thickness, as usual in AM applications. In this way, the indications that are obtained can be generalized to define AM design guidelines. The criteria that were adopted to choose the geometries and dimensions of specimens in this study can be summarized as follows:

- The use of classical and easily measured geometries;
- Thin walled sections;
- Flat surfaces;
- Open and closed sections;
- Alignment along the building direction (z–axis) or along the normal;
- Surfaces large enough to allow the strain gauges to be installed for the tests without suffering from edge effects due to the presence of sharp edges.

The following geometries were identified on the basis of the aforementioned criteria:

- Specimen A - a thin wall, with a thickness of 3 mm and sides of 20 mm and 30 mm, respectively, parallel to the building platform;
- Specimen B - a thin wall, with a thickness of 3 mm and sides of 20 mm and 30 mm, respectively, inclined 15 deg to the building platform;
- Specimen C - a thin wall, with a thickness of 3 mm and sides of 20 mm and 30 mm, respectively, inclined 30 deg

Table 1. Mean values of the tensile properties of aluminum alloy DMLS specimens along different orientations.

Orientation	Yield Strength $\sigma_{0.2}$ (MPa)	Ultimate Tensile Strength σ_{UTS} (MPa)	Elongation at break (%)
xy-plane	243 ± 7	330 ± 3	6.2 ± 0.3
z-axis	231 ± 3	329 ± 2	4.1 ± 0.2

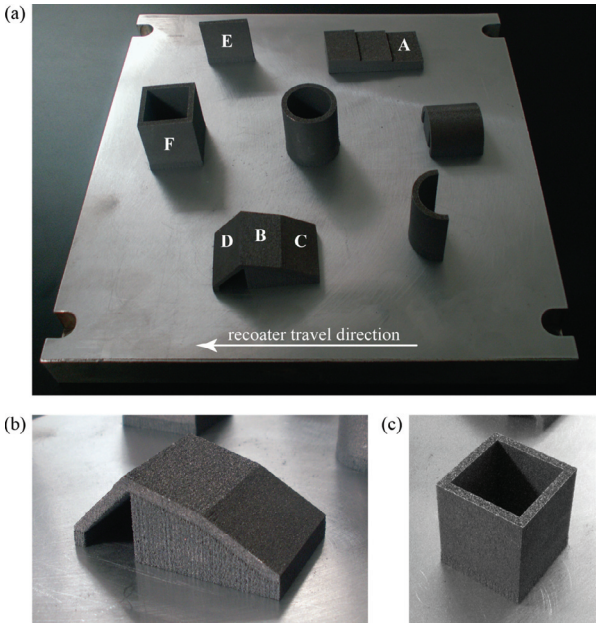

Fig. 2. (a) Construction platform with the samples after the heat treatment; (b) detail of specimens B, C and D; (c) detail of specimen F.

to the building platform;

- Specimen D - a thin wall, with a thickness of 3 mm and sides equal to 20 mm and 30 mm, respectively, inclined 45 deg to the building platform;
- Specimen E - a thin wall, with a thickness of 3 mm, and with the width and height equal to 30 mm, built along the z axis;
- Specimen F - a cylindrical hollow square section specimen, with a side of 30 mm, a wall thickness of 3 mm and a height of 30 mm, built along the z axis.

2.3. Fabrication of the specimens

Aluminum alloy specimens were produced in a single job using an EOSINT M 270 Dual Mode machine. This type of machine uses a 200 W fiber laser, with a wavelength of 1060-1100 nm, focused on a 0.1 mm diameter to melt the metallic powder. The layer was 30 µm thick and the building platform was kept at 100 °C. The components were constructed while blowing Argon into the work chamber in order to avoid oxidation of the material. A standard scanning strategy, which foresees different exposition parameters for the core, the skin, and the contour, was adopted [20].

The samples were fabricated using a saw-toothed 5 mm high support structure which connects them to the platform, in order to facilitate their removal. Moreover, the samples were orientated onto the platform at an inclination of 5 deg to the direction of the movement of the recoater blade (x-axis of the machine). This inclination was chosen in order to optimize the process and to avoid jamming of the recoater during the powder deposition phase so as to prevent the recoater from encountering on its entire length untreated zones of the previous layer. Moreover, the A, B and C specimens required a support structure, because of their alignment to the building platform (Fig. 2). After the construction, the platform with the samples was subjected to a stress relieving thermal treatment at 310 °C for 1 hour. The specimens were then removed from the platform and a surface shot-peening process was conducted. A NORBLAST shot-peening machine was used for the shot-peening treatment, utilizing spherical corundum particles at a pressure of 2 bar. A 6 mm nozzle was kept inclined at 45 deg to the treated surface.

2.4. Evaluation of the residual stresses

After shot-peening treatment operation, the samples were measured in order to evaluate the residual stress distribution. An MTS3000 RESTAN system by SINT Technology (Fig. 3), which is based on the hole drilling strain gauge method, was used to measure the residual stresses [19]. The hole-drilling method is a standardized method that allows accurate experimental stress analysis to be conducted, and it is one of the most efficient semi-destructive modes for the detection of residual stresses, in terms of costs, accuracy and versatility. The strains released by the tested material are acquired for each drilling step, and are used to calculate the residual stresses according to the ASTM E837-13a standard [19]. A 2 mm diameter drill bit is used to produce a 1.2 mm deep flat-bottom hole, through a sequence of 24 drilling steps of 50 µm. A K-RY61-1.5/120R rosette strain gauge, made by HBM, was utilized during the experimental campaign. The surface of the specimens, which presents a high level of roughness after the construction, was prepared for the application of the rosette strain gauge through sanding with a 200 grain abrasive paper and then with a 400 grain abrasive paper, Finally it was cleaned with an RMS1 spray solvent made by HBM. Fig. 3 shows specimen E during the test. The program for the calculation of the residual stresses from the measurement data was developed entirely in MATLAB R2009a, and the trend of the residual stresses in the thickness of the sample was evaluated by means of the Integral Method, as suggested in the ASTM E837-13a standard [19].

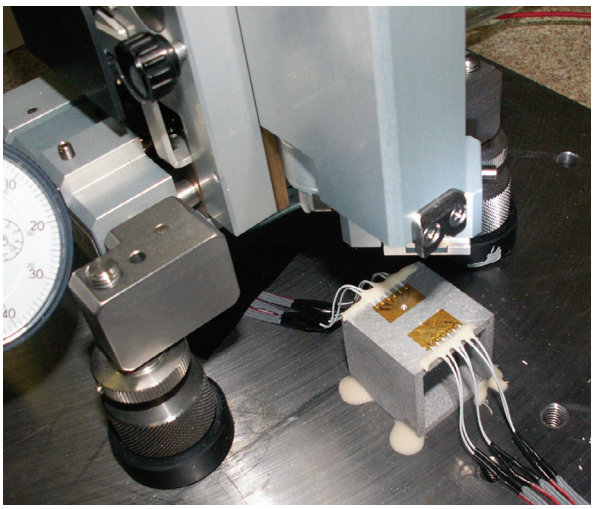

Fig. 3. MTS3000 RESTAN (REsidual STress ANalyzer) system by SINT Technology during a measurement phase on specimen E.

3. Results and discussion

The results of the residual stresses measurements are presented hereafter. The evolution of the stress profile of the samples is illustrated in function of the geometry of the specimens, in terms of orientations and open/closed sections.

3.1. Effect of the orientation

The residual stress distributions of the flat specimens, obtained with different inclinations, between 0 and 90 deg, are shown in Fig. 4 in function of the depth. These specimens are indicated with the letters A (0 deg), B (15 deg), C (30 deg), D (45 deg) and E (90 deg). It should be pointed out that the specimens with an inclination of less than 45 deg to the platform required a support system during the construction phase, and only specimens D and E are therefore self-supporting. All the specimens have shown a surface compression state. The behavior of specimens B, C, D and E was similar, and was characterized by a compression state to a depth of about 0.1 mm from the surface. This state of compression was probably generated by the surface shot peening treatment that was carried out on the surface of the specimens. A tensile state has been be observed at greater depths. This tensile state is characterized by an oscillating trend that becomes more marked as the inclination increases. This stress behavior is due to the fact that the residual stresses generated during the L-PBF process are the sum of the stresses due to hardening phenomena, derived from the solidification of the deposited layers, and of the thermal stresses due to the lack of correspondence between the thermal expansion and the stiffness of the different layers of the material during the process. The oscillating trend of the stresses is similar to the trend of the residual stresses that develop during a multi-pass welding process [22,23].

The maximum stress values, which do not exceed 75 MPa, are slightly higher in the D and E specimens, that is, in the self-supporting ones. The supports in fact constitute a thermal exchange surface with the higher thermal exchange coefficient of the unsintered powder, and therefore allow heat to be drawn out, the thermal gradient to be reduced and, as a result, the residual stress state is also reduced. The tensile stress state in specimen E, which grew along the vertical direction, cancels out at a depth of about 0.7 mm. The tension in specimens B, C and D instead reduces in the measured field to a minimum value, but without disappearing completely. Although the stress state in specimens B, C and D is measured from the upper wall of the specimen going, though at an inclination, toward the platform, the stress state in specimen E is measured on the build layer, from the skin to the core. It is possible that the behavior of this specimen is different from that of the other specimens as it has to wait to be symmetrical with the central axis of the specimen itself. Specimen A shows a different kind of behavior from that of the other specimens: the residual stress state is almost nil and the compression is present to almost half of the analyzed depth. This different behavior is probably due to the fact that the specimen is at a distance of only 5 mm from the construction platform, to which it is connected by supports, and that the construction platform is kept at a temperature of 100 °C. In this condition, the thermal gradients are much lower than in the other analyzed cases, and this can explain the different stress distribution.

The value of angle β, which describes the main direction of the stresses in function of the depth (Fig. 5a), is about 50 deg, whether positive or negative, except for specimen C, for which the β angle is equal to 0 deg. The β angle is the angle between gauge 1 and the principal stress direction (Fig. 5b), which means that the direction of the principal stress with respect to direction x (recoater travel direction) is equal to $\alpha = \beta + 40$ deg, for the chosen type of rosette, considering that it is applied along the width of the component, that is in turn built with an orientation of 5 deg with respect to the recoating direction. In short, the tendencies that can be observed show that the principal stress occurs along the specimen plane aligned to the x axis (specimens A, B and E), in a perpendicular direction (specimen D) or at 45 deg (specimen C). Abrupt variations in the values can be observed when the distribution curve of the stresses crosses the zero line, and the tensile stress state inverts to a compression stress state, or vice versa.

3.2. Open and closed sections

As far as specimens E and F are concerned, which are developed along the vertical direction, the strain gauge rosettes were installed both in the lower part of the specimen,

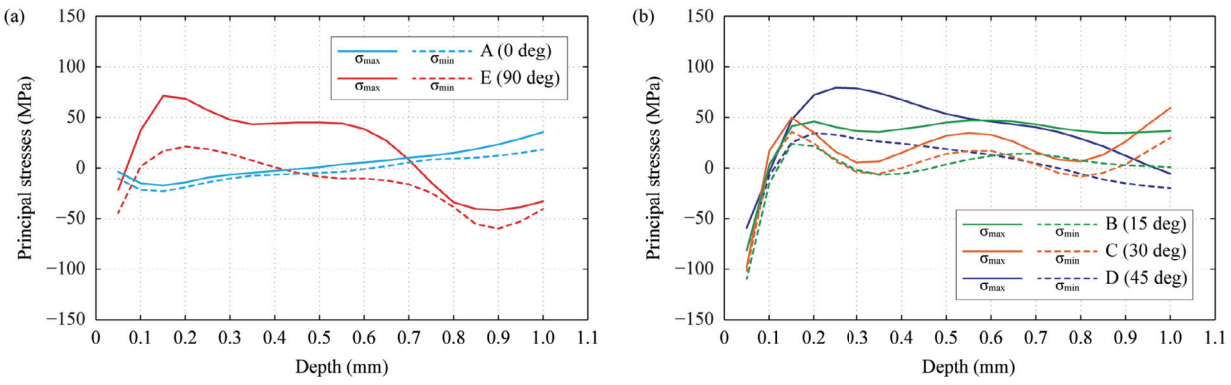

Fig. 4. Residual stress distributions of the open-section flat specimens; (a) A and E specimens; (b) B, C and D specimens.

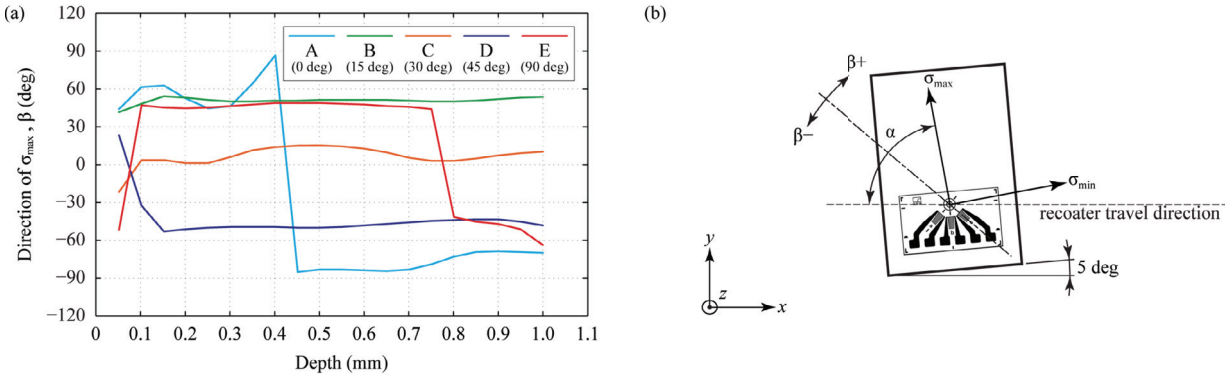

Fig. 5. Trend of the β angle on the open-section flat specimens and (b) arrangement of the rosette (top view) on the horizontal flat specimens.

in order to keep the same measurement distance from the platform as that of the other specimens, and in the upper part of the specimens, in order to evaluate the effect of the distance from the building platform. It is in fact known from the literature that the residual stress state is greater moving away from the construction platform, as the thermal effect generated by heating of the platform itself is reduced [21]. For specimens E and F, the distances of the measurement points from the building platform were 15 and 25 mm, considering the support height of 5 mm. Results show that a distance increase of 10 mm from the building platform does not significantly alter the stress state distribution for the considered geometries.

The two specimens show a similar trend for the β angle, respect to the depth. Nor the open/closed section or the distance from the building platform significantly affect the β angle behavior. The direction of the principal stress σ_{max} is approximately 45° and consequently the principal stress is normal to the x-axis of the machine. A sharp variation in the value of the β angle is detected at a depth of about 0.8 mm, which corresponds to the sign change of the principal stresses. In other words, the value of β steeply changes when a variation is observed in terms of principal stresses from a tensile stress state to a compression stress state.

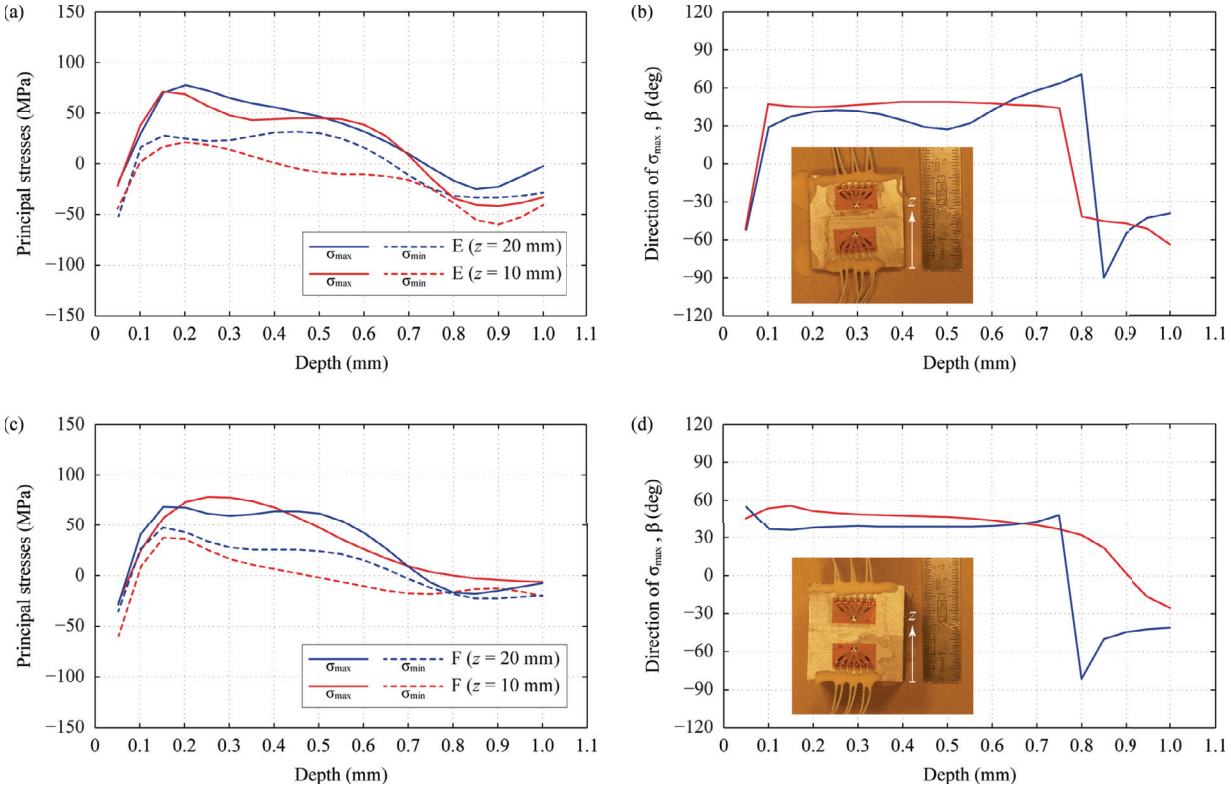

Fig. 6. (a) Residual stress distributions and (b) trend of the β angle at two different heights along building direction of the open-section specimen E; (c) residual stress distributions and (d) trend of the β angle at two different heights along building direction of the closed-section specimen F.

4. Conclusions

The experimental study described in this paper has made it possible to show that a residual compression stress state is realized on the surface of AlSil0Mg specimens produced by means of the L-PBF process, after a thermal and a shot peening treatment, to a depth of about 0.1 mm. Below this compressed layer, the stress state is prevalently of a tension type in the considered measured depth, that is, to 1 mm, and it shows an oscillating trend. The maximum stress is always below 100 MPa. Although this trend has been observed on different specimens, a variation in the reached maximum stress value has been noted when the geometrical conditions have been changed, but variations in this stress have also been observed as the depth increases. The factors that play a role are above all the presence or lack of supports and the geometry of the specimen, whether closed or open. Supports favor the transfer of heat during the construction process, and gradually reduce the stress state. Moreover, the residual stress is lower in the case of a free geometry, in that there is a greater possibility of stress release than in the closed geometry case. A different kind of behavior of the stress distribution has also been observed between the flat horizontal specimen and the vertical one: in fact, the part in tension in the latter is confined to a shallower depth, probably because of the axial symmetry of the 3 mm thick specimen, as the residual stresses are self-equilibrated.

Acknowledgements

The authors would like to thank Mr. Giovanni Marchiandi and Dr. Alessio Fiorentino for their assistance during the measurement phase and data elaboration. Moreover, the authors would also like to extend their thanks to Dr. Flaviana Calignano (Istituto Italiano di Tecnologia, Center for Sustainable Future Technologies CSFT@Polito, Torino, Italy) for her help in specimens fabrication.

References

[1] Atzeni E, Salmi A. Economics of additive manufacturing for end-usable metal parts. The International Journal of Advanced Manufacturing Technology. 2012;62:1147-55.
[2] Calignano F, Manfredi D, Ambrosio EP, Biamino S, Lombardi M, Atzeni E, Salmi A, Minetola P, Iuliano L, Fino P. Overview on Additive Manufacturing Technologies. Proceedings of the IEEE. 2017:1-20.
[3] Chen Y, Sheng IC. Residual Stress in Weldment. Journal of Thermal Stresses. 1992;15:53-69.
[4] Yilbas BS, Akhtar SS. Laser bending of metal sheet and thermal stress analysis. Optics & Laser Technology. 2014;61:34-44.
[5] Kempen K, Vrancken B, Buls S, Thijs L, Van Humbeeck J, Kruth JP. Selective Laser Melting of Crack-Free High Density M2 High Speed Steel Parts by Baseplate Preheating. J Manuf Sci E-T Asme. 2014;136.
[6] Alimardani M, Toyserkani E, Huissoon JP, Paul CP. On the delamination and crack formation in a thin wall fabricated using laser solid freeform fabrication process: An experimental–numerical investigation. Optics and Lasers in Engineering. 2009;47:1160-8.
[7] Olakanmi EO, Cochrane RF, Dalgarno KW. A review on selective laser sintering/melting (SLS/SLM) of aluminium alloy powders: Processing, microstructure, and properties. Prog Mater Sci. 2015;74:401-77.
[8] Vrancken B, Cain V, Knutsen R, Van Humbeeck J. Residual stress via the contour method in compact tension specimens produced via selective laser melting. Scripta Materialia. 2014;87:29-32.
[9] Sames WJ, List FA, Pannala S, Dehoff RR, Babu SS. The metallurgy and processing science of metal additive manufacturing. International Materials Reviews. 2016;61:315-60.
[10] Mercelis P, Kruth JP. Residual stresses in selective laser sintering and selective laser melting. Rapid Prototyping J. 2006;12:254-65.
[11] Gusarov AV, Pavlov M, Smurov I. Residual Stresses at Laser Surface Remelting and Additive Manufacturing. Lasers in Manufacturing 2011: Proceedings of the Sixth International Wlt Conference on Lasers in Manufacturing2011. p. 248-54.
[12] Cheng B, Shrestha S, Chou K. Stress and deformation evaluations of scanning strategy effect in selective laser melting. Additive Manufacturing. 2016;12, Part B:240-51.
[13] Lu Y, Wu S, Gan Y, Huang T, Yang C, Junjie L, Lin J. Study on the microstructure, mechanical property and residual stress of SLM Inconel-718 alloy manufactured by differing island scanning strategy. Optics & Laser Technology. 2015;75:197-206.
[14] Gu DD, Meiners W, Wissenbach K, Poprawe R. Laser additive manufacturing of metallic components: Materials, processes and mechanisms. International Materials Reviews. 2012;57:133-64.
[15] Ding J, Colegrove P, Mehnen J, Ganguly S, Almeida PMS, Wang F, Williams S. Thermo-mechanical analysis of Wire and Arc Additive Layer Manufacturing process on large multi-layer parts. Comp Mater Sci. 2011;50:3315-22.
[16] Griffith ML, Rogge RB, Holden TM, Rangaswamy P. Residual stresses in components formed by the laserengineered net shaping LENS (R) process. The Journal of Strain Analysis for Engineering Design. 2003;38:519-27.
[17] Rangaswamy P, Griffith ML, Prime MB, Holden TM, Rogge RB, Edwards JM, Sebring RJ. Residual stresses in LENS (R) components using neutron diffraction and contour method. Mat Sci Eng a-Struct. 2005;399:72-83.
[18] Kruth JP, Deckers J, Yasa E, Wauthle R. Assessing and comparing influencing factors of residual stresses in selective laser melting using a novel analysis method. P I Mech Eng B-J Eng. 2012;226:980-91.
[19] ASTM E837-13a, Standard Test Method for Determining Residual Stresses by the Hole-Drilling Strain-Gage Method, ASTM International, West Conshohocken, PA, 2013, http://www.astm.org/.
[20] Manfredi D, Calignano F, Krishnan M, Canali R, Ambrosio E, Atzeni E. From Powders to Dense Metal Parts: Characterization of a Commercial AlSiMg Alloy Processed through Direct Metal Laser Sintering. Materials. 2013;6:856-69.
[21] Atzeni E, Salmi A, Galati M, Iuliano L. Experimental analysis of residual stresses on AlSi10Mg parts produced by means of Selective Laser Melting (SLM). 10th CIRP Conference on Intelligent Computation in Manufacturing Engineering - CIRP ICME '16. Ischia (Naples), Italy: Elsevier B.V; 2016.
[22] Teng T-L, Chang P-H, Tseng W-C. Effect of welding sequences on residual stresses. Computers & Structures. 2003;81:273-86.
[23] Chiumenti M, Cervera M, Salmi A, Agelet de Saracibar C, Dialami N, Matsui K. Finite element modeling of multi-pass welding and shaped metal deposition processes. Computer Methods in Applied Mechanics and Engineering. 2010;199:2343-59.